RESULTS AND DISCUSSION

Results and Discussion

The composition of tin(IV) antimonate prepared was (Sn/Sb) 0.7 and it is yellow in color. The molar ratio of the Sn/Sb in the precipitate approached the same ratio as in the initial mixed solution, when the hydrolysis was carried out with a large amount of water at higher temperature [1].

1-XRD analysis:

The Powder X-ray diffraction patterns, made for material precipitated showed that it may contain amorphous antimonic acid (A-Sb-A) and α-tin(IV) hydrous oxide. It is very difficult to identify the presence of A-Sb-A in the sample by X-ray diffraction analysis. Figure 8 a,b,c, shows the XRD for the SnSb samples heated at different temperatures (50, 200, 400°C) up to 6 hours, respectively. The patterns show a slight increase in the crystallinity and this can be interpreted as the formation of Sb_6O_{13} and SnO_2 which have sharp XRD patterns. Figure 8-d shows the pattern of the sample heated at 50°C and saturated with europium nitrate at room temperature. The non-deformation of the pattern according to the exchange process indicates that the stability of the compound as an exchanger.

2-Water content:

The water content of the prepared sample was determined by

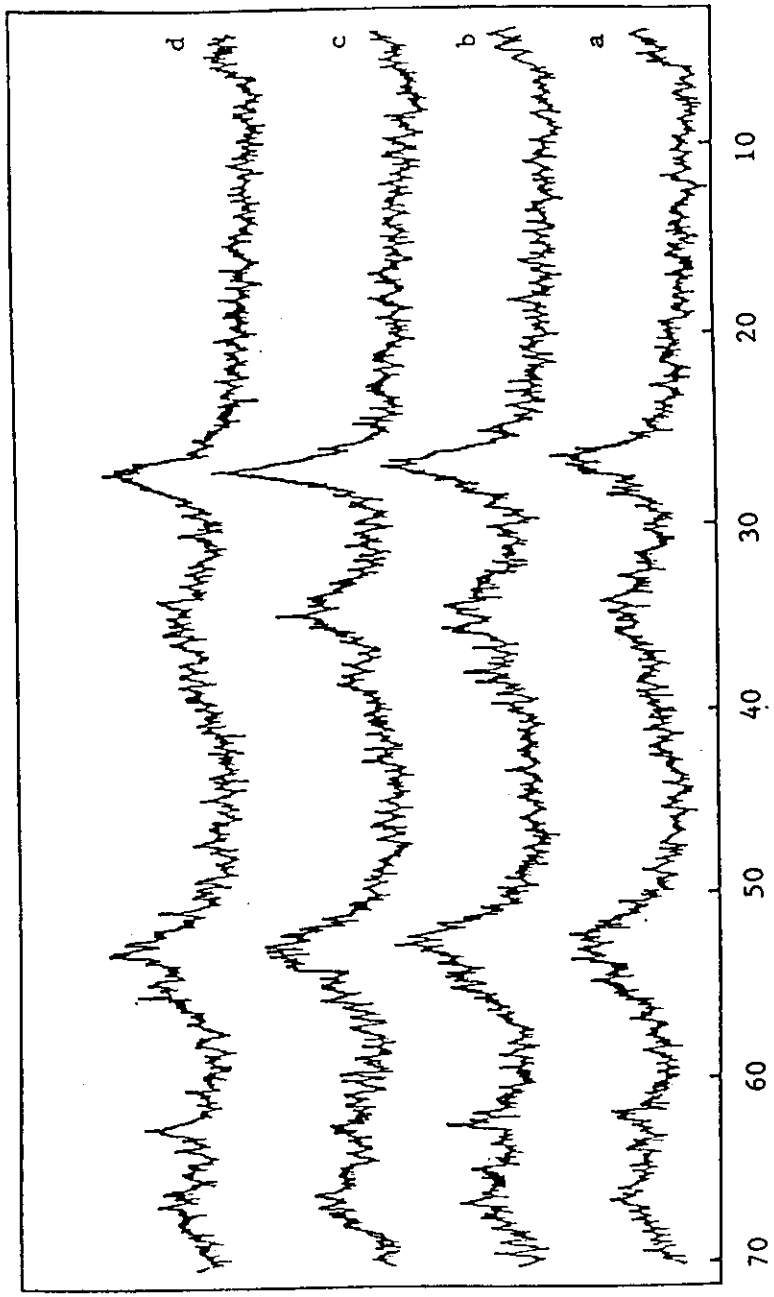

Fif. 8: XRD powder pattern of SnSb heated at; a: 50°C, b: 200°C, c: 400°C and d: at 50°C saturated with europium.

calcination at 850°C in air for 24 hours and it was found to be 13.7%.3-Thermal analysis:

The thermal-gravimetric and differential thermal analysis curves are given in Figure 9. The first endothermic peak in the DTA curve is broad and the weight loss continued upto 600°C. These results indicate that the SnSb has a good thermal stability compared with the other inorganic ion exchangers, as reported by Qureshi et. al. [52].

The small exothermic peak at 320°C corresponding to the crystallization of SnO_2 [53], was not found and this is attributed to the high ratio of Sn/Sb. A small endothermic peak, accompanied with a weight loss at 590°C, may be due to the further condensation of the antimonic hydroxide groups, similar as in zirconium phosphate [212]. The sample did not show a weight loss beyond 600°C. By assumption that the sample composition at 600°C is $SnO_2.XSb_2O_5$, where the molar ratio Sn/Sb is 0.7 and the water content is 13.7%, the empirical formula for SnSbA can be established as $SnO_2.1.44Sb_2O_5.2.62H_2O$.

4-Infrared spectra:

The IR spectra of SnSb heated at different temperatures are given in Figure 10. The adsorption band in Figure 10-a at 3450 and 1600 cm^{-1} were assigned to be the stretching and deformation vibration of the interstitial water with strong hydrogen bonding. The band at 750 cm^{-1} is ascribed to Sb-O stretching vibration [212]. The broad band at 1100 cm^{-1} may be ascribed to SbOH.

With increasing the sample heating temperature at 200 and 400°C

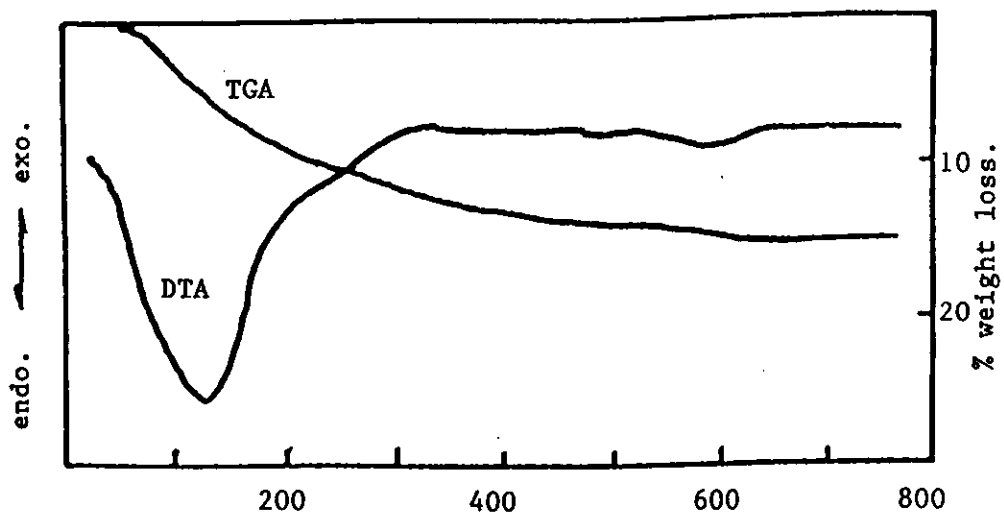

Fig. 9: TGA and DTA curves of tin(IV) antimonate used.

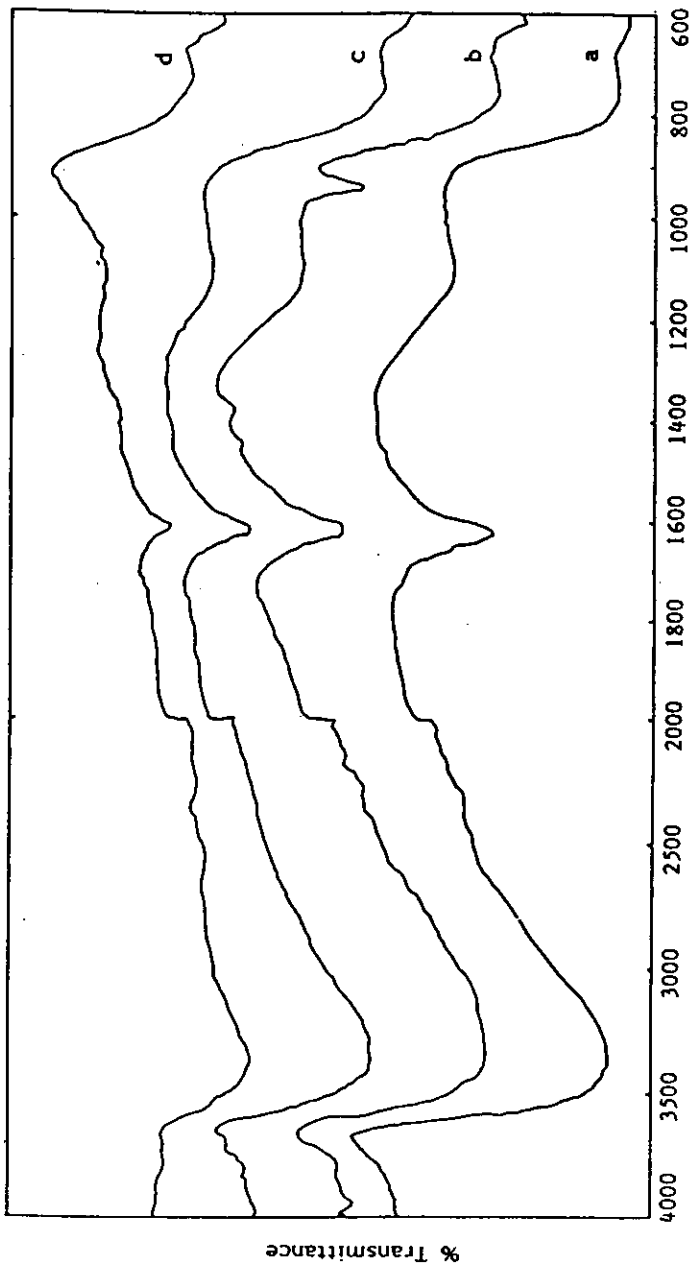

Fig. 10: IR spectra of SnSb heated at; a: 50°C, b: 50°C and loaded with uranyl ion, c: 200°C and 400°C.

Figure 10-c,d showed respectively the decrease in the adsorption bands at 3450, 1600 and 1100 cm^{-1} according to the decrease in water and -OH content in the sample. Figure 10-b shows the IR spectrum of the SnSb sample heated at 50°C and saturated with uranyl nitrate at room temperature. The spectrum showed a sharp beak at 930 cm^{-1} which is the adsorption band of uranyl ion. This gives evidence that the uranium was taken up as UO_2^{2+} replacing the H^+ in the interstitial water or the proton form the SbOH group. However, the curve did not show the nitrate group indicating the cation exchange behavior of the SnSb exchanger, inagreement with Abe [58].

To carry out a study of the ion exchange properties of SnSb the prepared uranyl and radioactive cobalt, and europium ions were selected to verify the different parameters. These elements are important in the nuclear fuel waste because they represent the corrosion of rare earth and actinide species.

Distribution coefficient, hydrogen ion concentration, kinetic equilibrium, particle size, temperature and concentration were studied for each element and the results given as follows.

5- Cobalt:

5.1- Distribution coefficient:

Sorption of 10^{-4}M cobalt at different acidities was determined at a V/m of 600 cm^3/g at 25°C. Figure 11, illustrates the dependence of the log K_d (distribution coefficient) vs. log hydrogen ion concentration in the aqueous phase. The slope was found to be almost one, however the ion

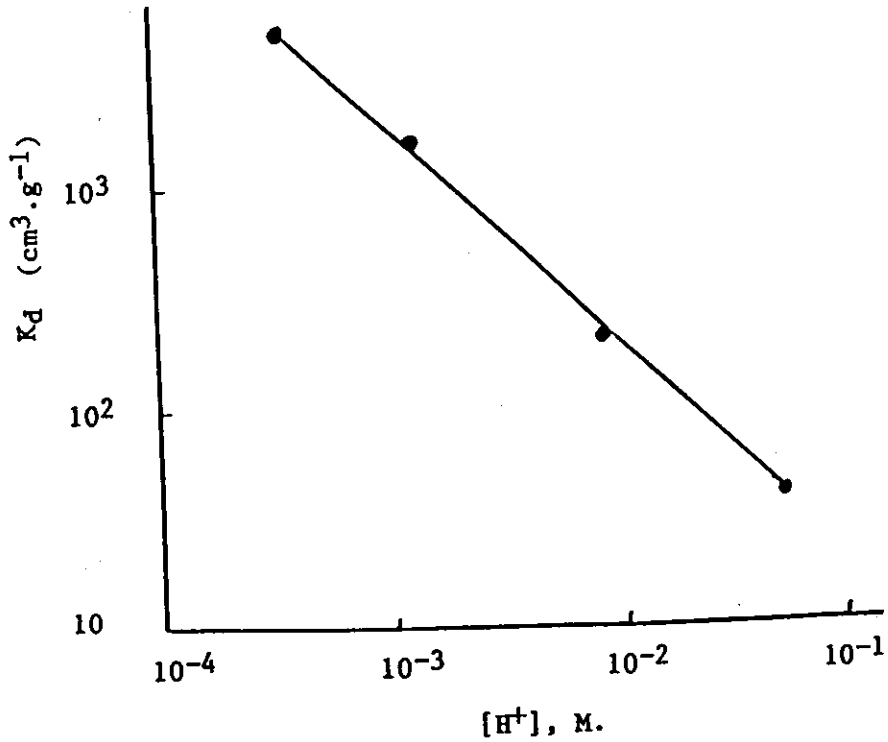

Fig. 11: Variation of K_d, with equilibrium $[H^+]$ ion for sorption of Co(II) ion, 10^{-4}M, at 25°C by SnSb (V/m=600 cm^3 g^1)

exchange reaction could be represented as follows:

$$mCo^{2+} + R.XH_2O = R.(OH)_mCo^{m+}(X\text{-}m)(HOH) + mH^+$$

where R stands for $SnO_2.Sb_2O_5$ and formulas with bars represent the solid phases.

From the slope of the straight in Figure 11, it can be concluded that, about one mole of hydrogen ion was released from the SnSb surface for each mole of metal ion adsorbed. Since the ratio of the charge released is less by one than that adsorbed so the adsorption of the metal ion should produce a decrease in the negative surface charge.

Figure 12, shows the effect of Co^{2+} concentration on the exchange capacity determined by standard batch technique [213], at pH 2. A constant value was obtained for Co^{2+} solutions greater than $5.0X10^{-3}M$. The batch reproducibility shows a standard deviation of 0.04. Also from Figure 12, it could be concluded that there is a steady decrease in the distribution coefficient with increase of metal ion concentration.

5.2- Kinetic of exchange:

The influence of particle radius and solution concentration on the rate of exchange are presented in Figure 13. The rate of cobalt ion uptake is markedly dependent on the particle size and independent of concentration, indicating particle diffusion controlled exchange for cobalt ion [214].

Figures 13-16, represents the plot of Bt vs. t and B vs. $1/r^2$ and Figure 17 shows a straight line whichconfirms the particle diffusion mechanism (Appendex II). The values of D_i calculated from Figures 13

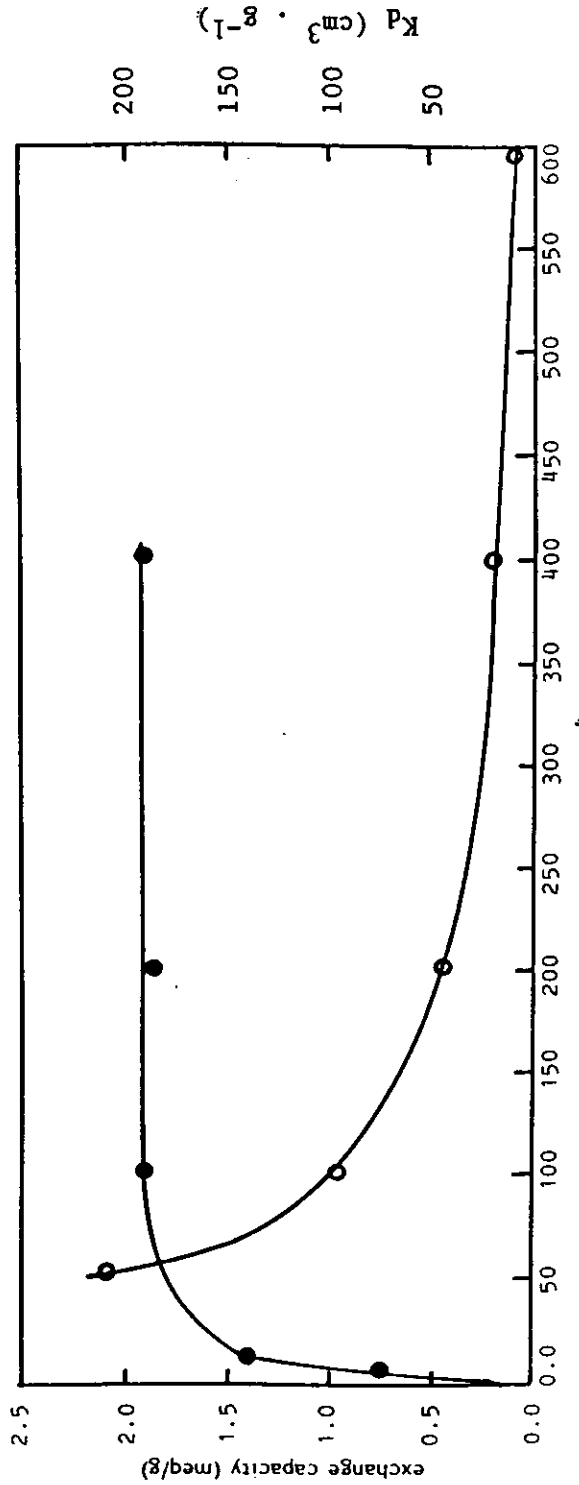

Fig. 12: Variation of Kd, ● and capacity O, with concentration of Co(II) ion at 25°C by SnSb at pH 2. (V/m=400 ml g^{-1}).

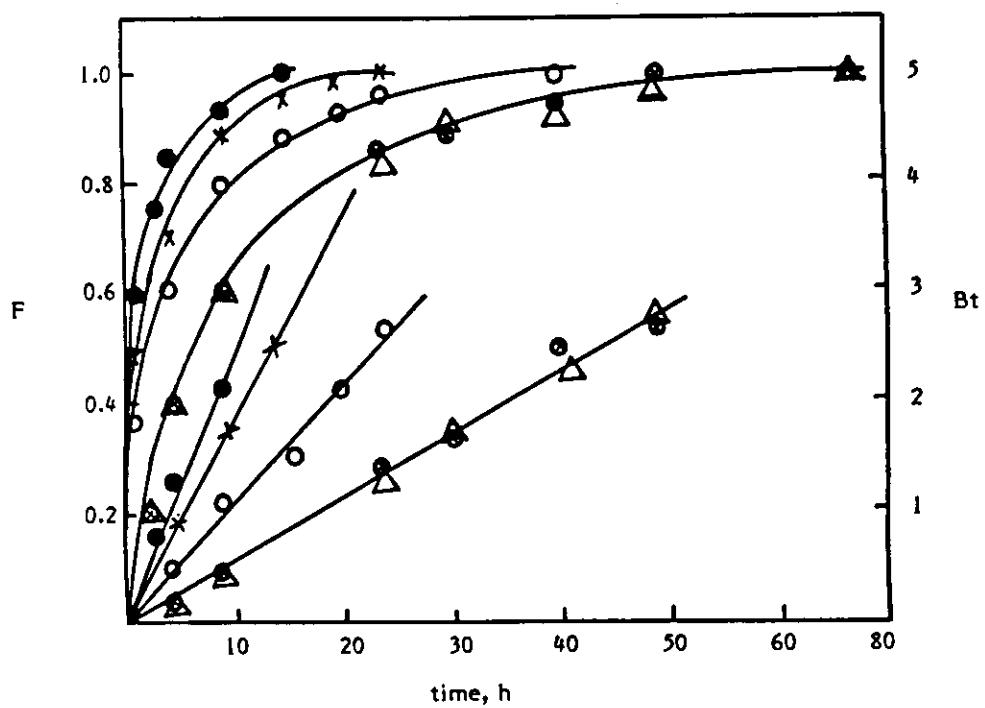

Fig. 13: Plots of F and Bt vs. time for exchange of Co(II) at 25°C at different concentrations and particle diameters: $5X10^{-3}$M, 0.45 mm, Δ; 10^{-2}M, 0.45 mm, ⊗, 10^{-2}M, 0.325 mm, ○; 10^{-2}M, 0.225 mm, χ; 10^{-2}M, 0.16 mm, ●.

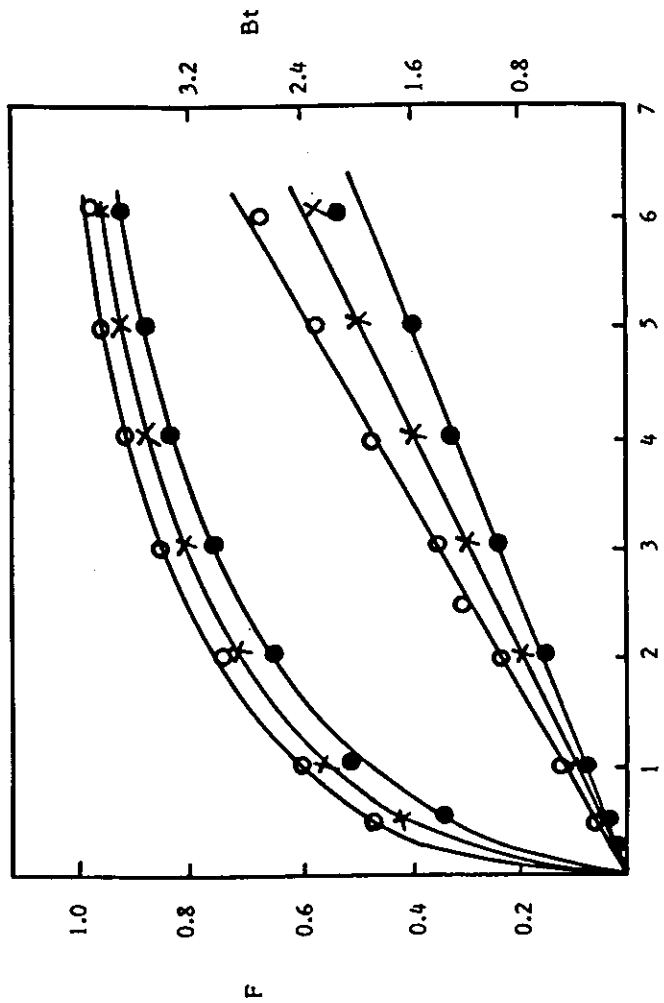

Fig. 14: Plots of F and Bt vs. time for exchange of Co(II) on SnSb dried at 50°C of particle diameter 0.16 mm; ●, 25°C; X, 45°C, O, 60°C.

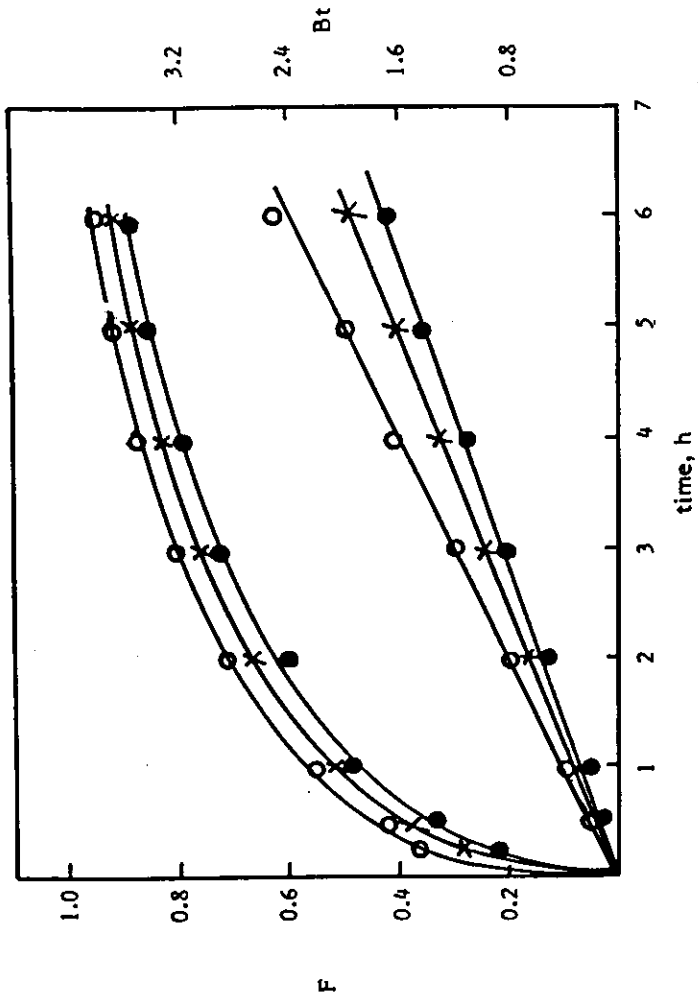

Fig. 15: Plots of F and Bt vs. time for exchange of Co(II) on SnSb heated at 200oC of particle diameter 0.16, ●, 25°C; X, 45°C, O, 60°C.

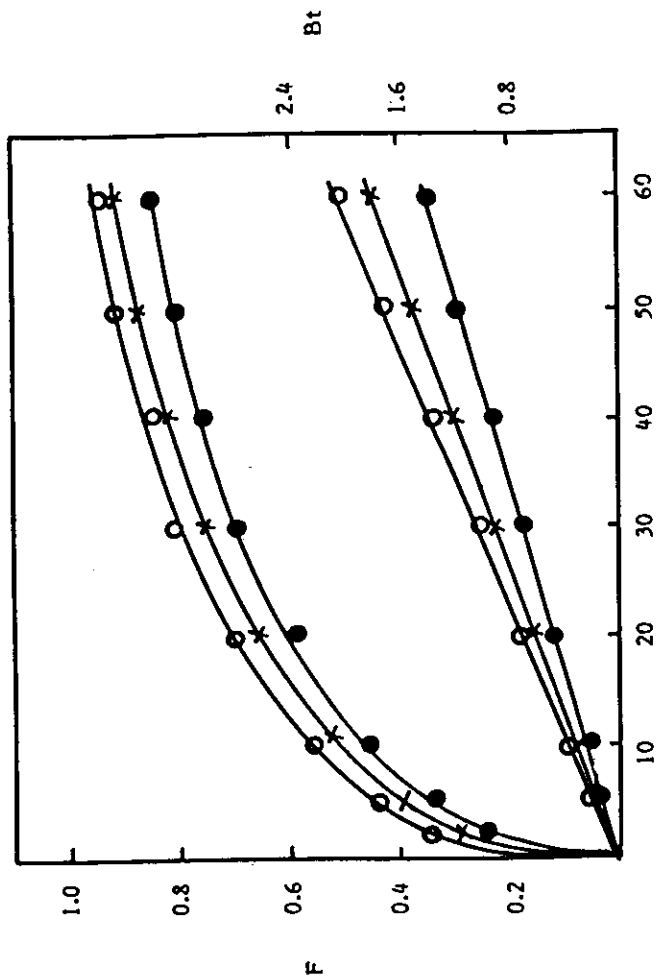

Fig. 16: Plots of F and Bt vs. time for exchange of Co(II) on SnSb heated at 400°C of particle diameter 0.16 mm, ●, 25°C; X, 45°C, O, 60°C.

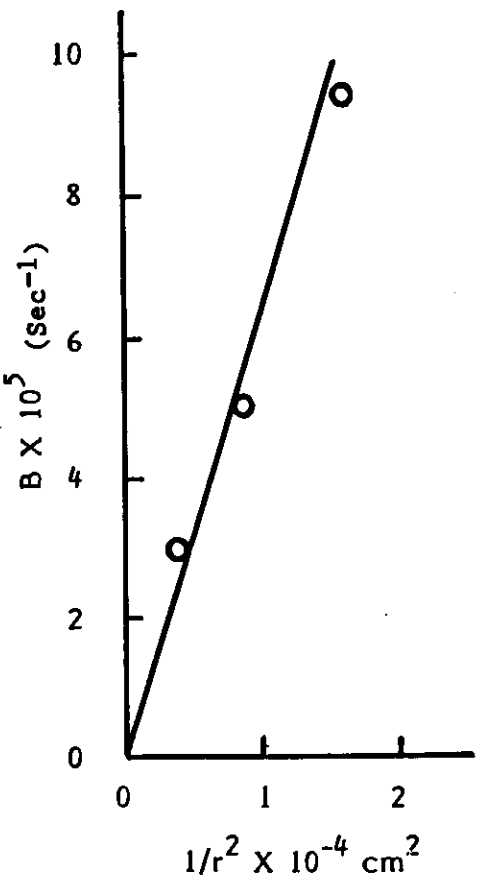

Fig. 17: Plot of B vs. $1/r^2$ for CO^{2+} at 25°C on SnSb.

Table 2: Values of D_i at 25°C for Co^{2+} exchange on tin(IV) antimonate of different particle size.

Heating Temp. °C	Particle diameter mm	$D_i X 10^{10}$ cm^2 S^{-1}
50	.16 .23 .33 .45	6.13 6.22 8.01 8.56
200	.16	5.05
400	.16	4.33

16, are given in Table 2. This table shows that the diffusion coefficients calculated for a larger particle size are slightly high. This difference is related to the possible agglomeration of smaller units and therefore a quicker diffusion took place through the channels between these units [215]. The higher D_i for a larger particle size was also reported by others [16].

The plots of Bt vs. t for the exchange of cobalt on the sample heated at 50, 200 and 400°C of particle diameter 0.16 mm are given in Figures 14-15. The calculated values of the effective diffusion coefficient are given in Table 2. The lower values of D_i Given for cobalt at higher heating temperatures may be attributed to the lower pore size and porosity. The lower porosity would mean less free water inside the structure, which hinders the ion diffusion [215]. Besides, on drying at higher temperature, interparticle condensation takes place with a subsequent growth in the primary particles which is frequently accompained by a marked structural ordering and an increase in crystallinity growth as confirmed by the sharpening of the reflection in the XRD pattern.Similar findings were determined [214,217,218].

Figures 14,15, illustrate the relation between Bt vs. t for the exchange of cobalt on the exchanger under investigation with a particle diameter 0.16 mm at the reaction temperatures 25, 45 and 60°C. From these Figures log D_i could be calculated (Appendex IV). However, Figure 18, shows a straight line when plotting log D_i vs. 1/T. Accordingly the activation energy was calculated and is given in Table 3.

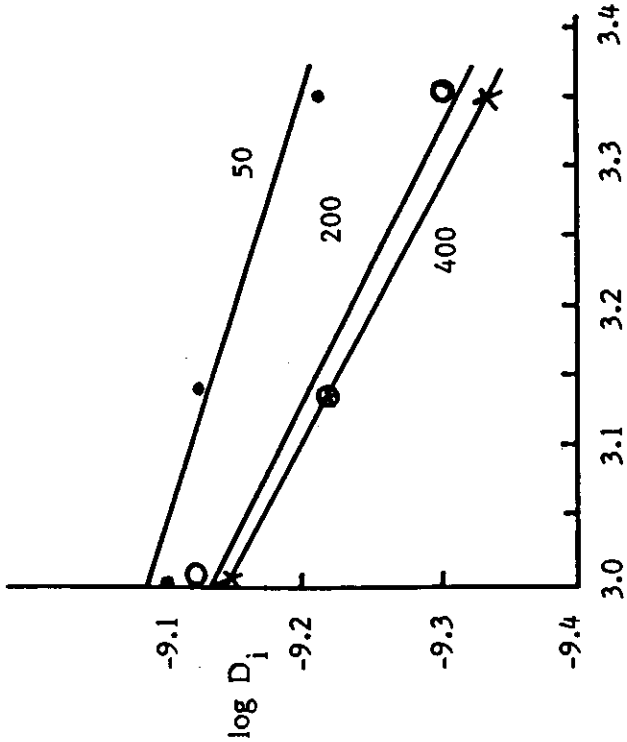

Fig. 18 : Arrhenius plots for exchange of Co^{2+} on SnSb heated at different temperatures particle diameter 0.16 mm.

Table 3: Values of B and activation energy (E_a) for exchange of Co^{+2} at different reaction temperatures on tin(IV) antimonate (heated at diff. temp.) of particle diameter 0.16 mm.

Heating temp. °C	Reaction temp. °C	B X10^5 cm^2 Sec^{-1}	E_a $KJ.mol^{-1}$
50	25	9.44	5.74
	45	11.10	
	60	12.12	
200	25	7.78	9.57
	45	8.89	
	60	11.11	
400	25	6.67	10.64
	45	9.01	
	60	10.00	

The lower values of the activation energies given in Table 3, support the particle diffusion controlled mechanism [219]. Also it is concluded that the activation energy for the oven dried samples are higher than the air dried one which may be due to the decrease of pore size as temperature increases, i.e the change in crystalline structure in water content of the sample implies a decrease in porosity [221].

5.3- Sorption isotherm:

The sorption isotherm results fit quite well the linear form of the Langmuir adsorption over the entire range of cobalt(II) investigated ($5.0X10^{-4}$ and $8.0X10^{-2}$M in 10^{-2}M HNO_3, at 25, 45 and 60°C).

From the Slope of the plots of C/w wv. C, Figure 19, the value of M, the saturation capacity of tin(IV) antimonate for cobalt (II) at the investigated temperature and pH=2, are 0.6, 0.57 and 0.45 meq/g, respectively. The results agree with the general range reported in the literature for several metal oxide inorganic exchangers [220-222].

Figure 20, is a plot of ln a vs. 1/T, accordingly the value of ΔH at saturation is calculated, (Appendix IV), for tin(IV) antimonate and it was found equal to -12.55 KJ mol^{-1}. This value indicates the indothermic behavior of tin(IV) antimonate. This exchange reaction is favorably when compared of with values of -62.37, 59.85, -66.97 and -26.37 KJ mol^{-1} for cobalt (II) adsorption on Al_2O_3, MnO_2, Fe_2O_3 and montmorillonite [221,223], respectively. This low value of ΔH in this study could be attributed to the fact that the synthetic tin(IV) antimonate might be easily hydroxylated (because it had not been subjected to temperatures higher

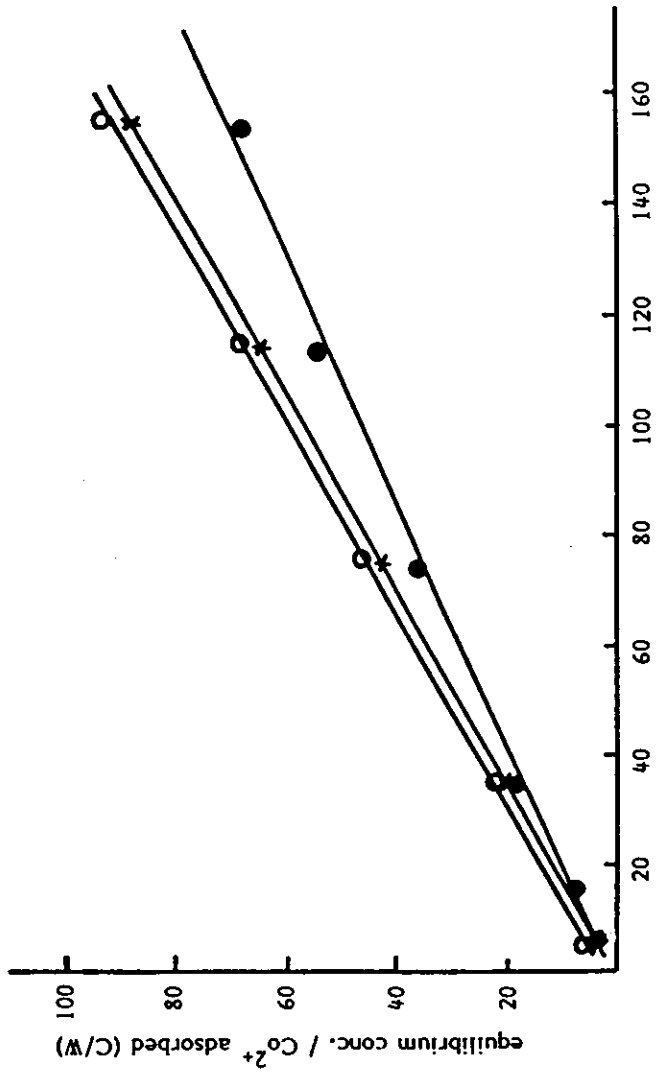

Fig. 19: Langmuir adsorption isotherm of Co(II) ion on SnSb at pH 2 and heated temperatures: O, 25°C; X, 45°C, ●, 60°C.

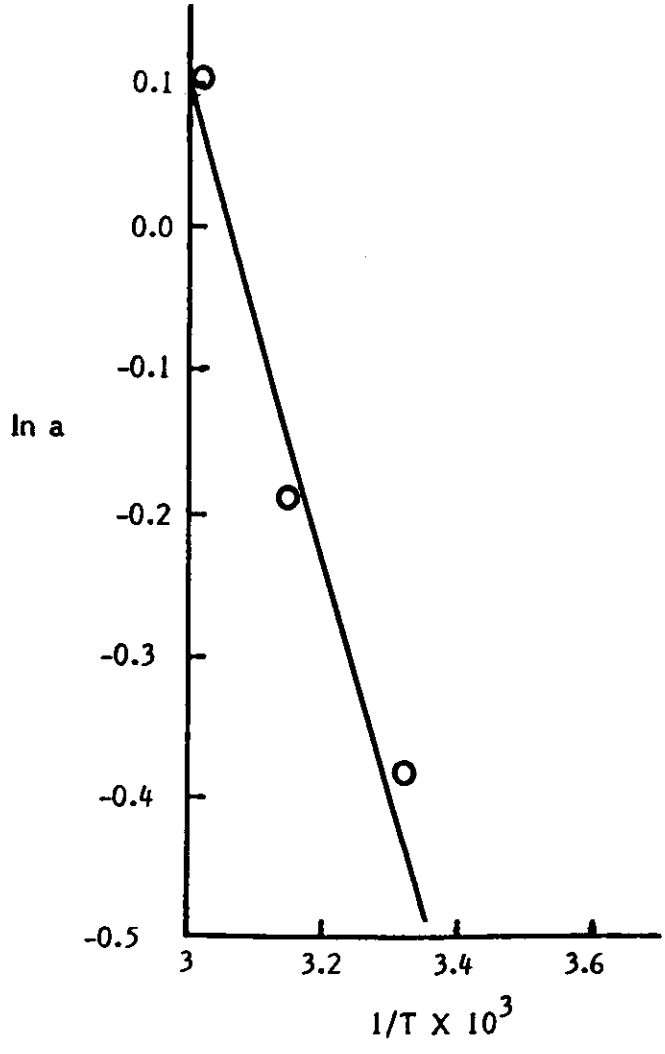

Fig. 20: Plot of ln a vs. 1/T for Co(II) adsorption on SnSb at pH 2.

SnSb at pH 2.

than 60°C) which might facilitate the surface reaction. In addition the decrease in the surface charge by the release of one mole of [H^+] resulting from the supposed weaker electrostatic interaction of cobalt(II) and tin(IV) antimonate which leads to the lower value of heat of adsorption.

6- Uranyl ion:

6.1- Equilibrium and pH measurements:

The equilibrium uptake of 10^{-3}M uranyl ion at different pH values on tin (IV) antimonate at 30°C is shown in Table 4, together with the initial and final (equilibrium) pH. On the assumption that within the pH range investigated, the sorption of uranyl ion occurs by cation exchange with H^+ ions, the final pH values of exchange were calculated Table 4. This assumption is based on the negligible hydrolysis of uranyl ion [224-226], and the absence of uranyl nitrate complex. From Table 4, it appears that the final pH values are very close to the calculated values. This indicates that cation exchange is most probably the main mechanism of uptake of uranyl ions by the matrix.(Appendix I)

6.2- Kinetics of exchange:

The results given in Figure 21, show that the exchange rate increases with the decrease in the particle size, where the effective diffusion coefficients are approximately constant, Table 5, which is in agreement with the fundamental conditions of particle diffusion. A plot of B vs. $1/r^2$, Figure 22, shows that the rate of exchange is inversely proportional to the particle size. With the increase in the heating

Table 4 : Sorption and pH variation for uptake of uranyl ions at 30°C from aqueous nitrate medium by SnSb

Initial con. (M)	V/m mlg^{-1}	% uptake	Initial pH	Final pH*	Calculated final pH
10^{-3}	200	18.27	1.00	1.11	0.998
		31.32	1.50	1.51	1.491
		49.00	2.05	2.03	2.005
		59.05	2.50	2.41	2.362
		66.60	2.80	2.60	2.540

* pH after equilibrium.

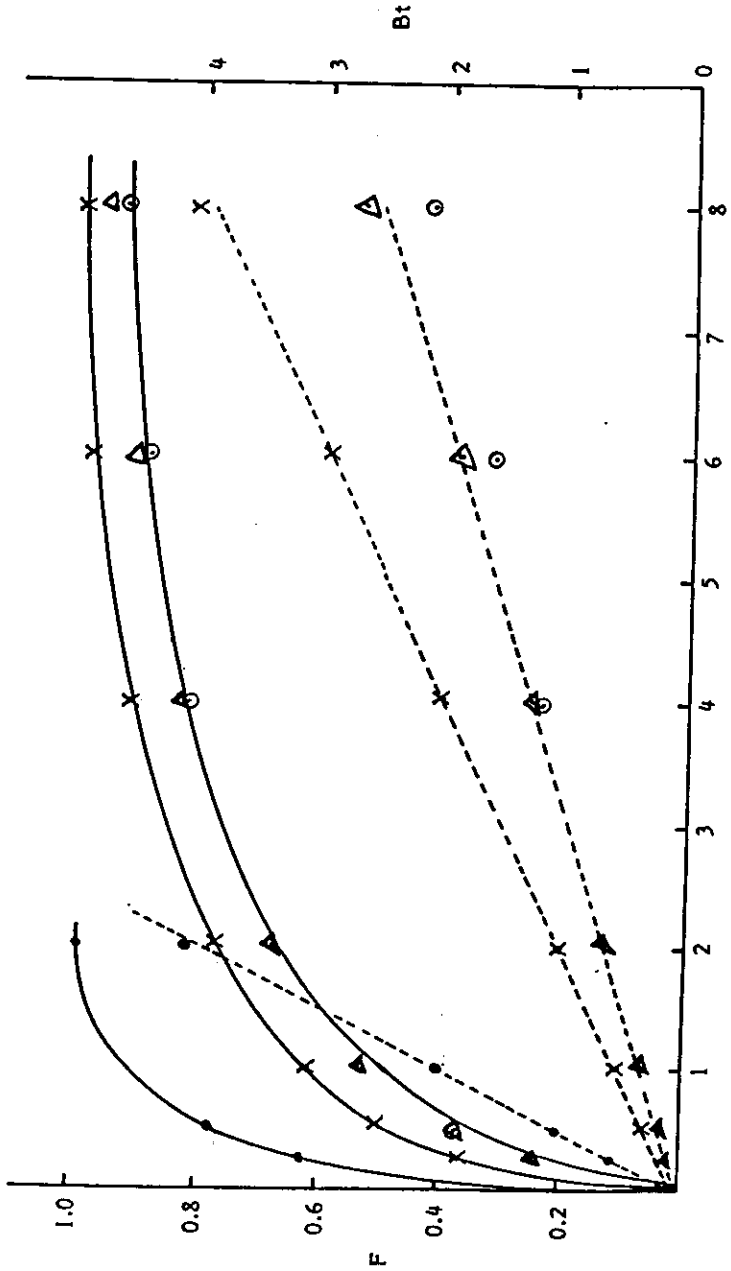

Fig. 21: Plots of F (solid line) and Bt (dashed line) vs. time for exchange of uranyl ion at 30°C a different concentrations and particle diameters, ⊙, 10^{-3} M, 0.4 mm;Δ,$5x10^{-3}$ M, 0.4 mm; X, 10^{-3} M, 0.32 mm; ●, 10^{-3} M, 0.16 mm.

Table 5 : Effective diffusion coefficients and other thermodynamic parameters calculated for exchange of uranyl ion on tin(IV) antimonate of particle diameter 0.4 mm

System	Diff. coeff. D_i cm^2/s			D_0	E_a	ΔS^*
	30°C	45°C	60°C	cm^2/s	kJ/mol	Jmol^{-1}K^{-1}
UO_2^{2+}/H^+	3.5×10^{-9}	7.9×10^{-9}	1.5×10^{-8}	1.09	35.9	−163.75

temperature of the exchanger from 50 to 400°C, an appreciable increase of (D_i) was observed, Table 5. This can be related to the increase in the crystallinity of SnSb with increasing temperature as observed from the XRD diffraction patterns. By increasing temperature, a gradual growth of SnSb particles is expected with possible increase in pore volume. This idea is supported by the work of Nancollas [214], who observed an increase of the effective diffusion coefficient of sodium ions on hydrous thorium dioxide with increasing crystallinity of the matrix.

The value of (D_i) calculated from the slopes of Bt vs. t plots for the exchange of uranyl ion on SnSb of 0.4 mm particles at the reaction temperatures 30, 45 and 60°C are given in Table 6. When log D_i was plotted against 1/T Figure 23, a straight line was obtained, enabling the estimation of the energy of activation (E_a) and the pre-exponentional constant (D_o) in the Arrhenius equation. The entropy of activation (ΔS^*) can then be calculated from D_o by use of the equation proposed by Barrer et. al. [227] (Appendix IV).

The values of interdiffusion coefficient (D_i), activation energy (E_a) and entropy of activation (ΔS^*) are given in Table 5. The entropy of exchange depends on the extent of hydration of the ions exchanged along with the change in water structure around the ions which may occur when they pass through the channels of the exchanger particles. The negative value of (ΔS^*) indicates a certain degree of dehydration of the cation with diffusing into the solid phase. In addition, the negative value of the entropy of activation suggest that by the exchange of this cation, no

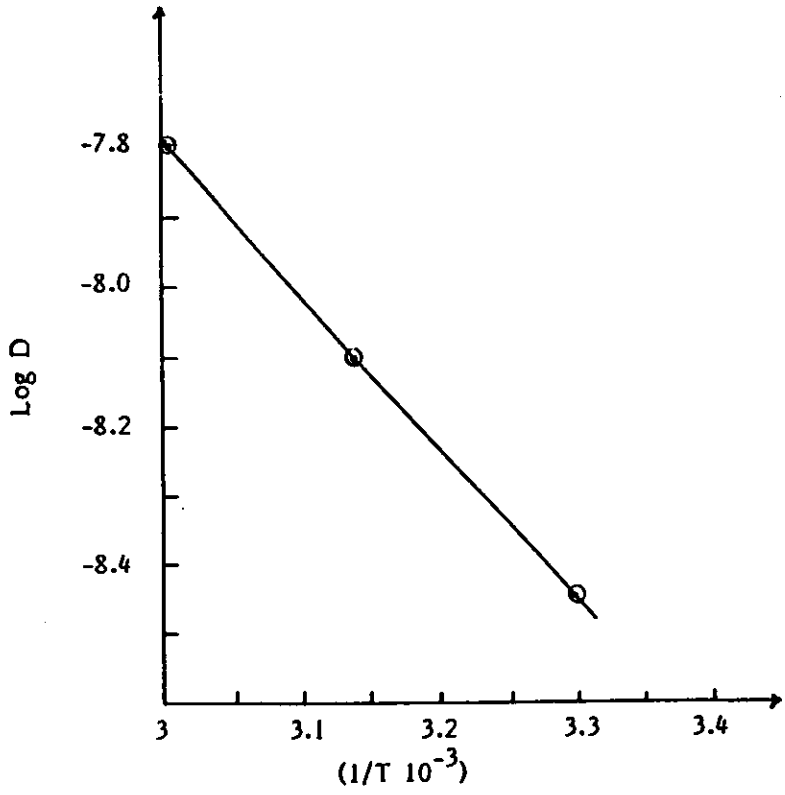

Fig. 23: Arrhenius plot for exchange of uranyl ion on SnSb of particle diameter 0.4 mm.

Table 6: Effective diffusion coefficients for exchange of uranium by tin(IV) antimonate at 30°C

Heating temp. °C	Conc. of salt (M)	Particle diameter (mm)	$D_i \times 10^9$ cm^2s^{-1}
50	10^{-3}	0.40	3.51
50	5×10^{-3}	0.40	3.51
50	10^{-3}	0.32	3.60
50	10^{-3}	0.16	3.60
200	10^{-3}	0.40	6.44
400	10^{-3}	0.40	31.20

significant structural changes occur.

6.3- Sorption isotherm:

The results were analyzed by use of the Langmuir adsorption isotherm. Langmuir plots, Figure 24, show the conformity of the data with the Langmuir equation. From the slope of the linear plots of C/w vs. C, the values of M, the saturation capacity for the adsorption has been determined (Appendix III). The saturation capacities of SnSb for uranyl ion at 30, 45 and 60°C at pH 2 are 0.5, 0.6 and 0.6 meq/g, respectively. El-Naggar [228] found no change in adsorption of uranyl ion on hydrous tin oxide over the temperature range 10-40°C. Mahal et. al. [158] reported that the sorption of uranium from nitrate solution on some hydrous oxides decreases with increase of temperature. An increase in sorption with temperature has also been found for polymers on glass, steel, and polyvinylchloride [229].

From the plot of ln a vs. 1/T, Figure 25, the value of ΔH is calculated. The heat of sorption calculated for SnSb was found to be -55.4 KJ mol^{-1}. The heat of sorption of uranium at saturation for hydrous TiO_2 and CeO_2 were reported to be -21.9 and -34.6 KJ mol^{-1}, respectively. The higher $-\Delta H$ value for SnSb may be due to the unhydroxylated surface of tin (IV) antimonate in comparison with other hydrous oxides. This is expected to retard the surface reaction (film diffusion) for SnSb as found above.

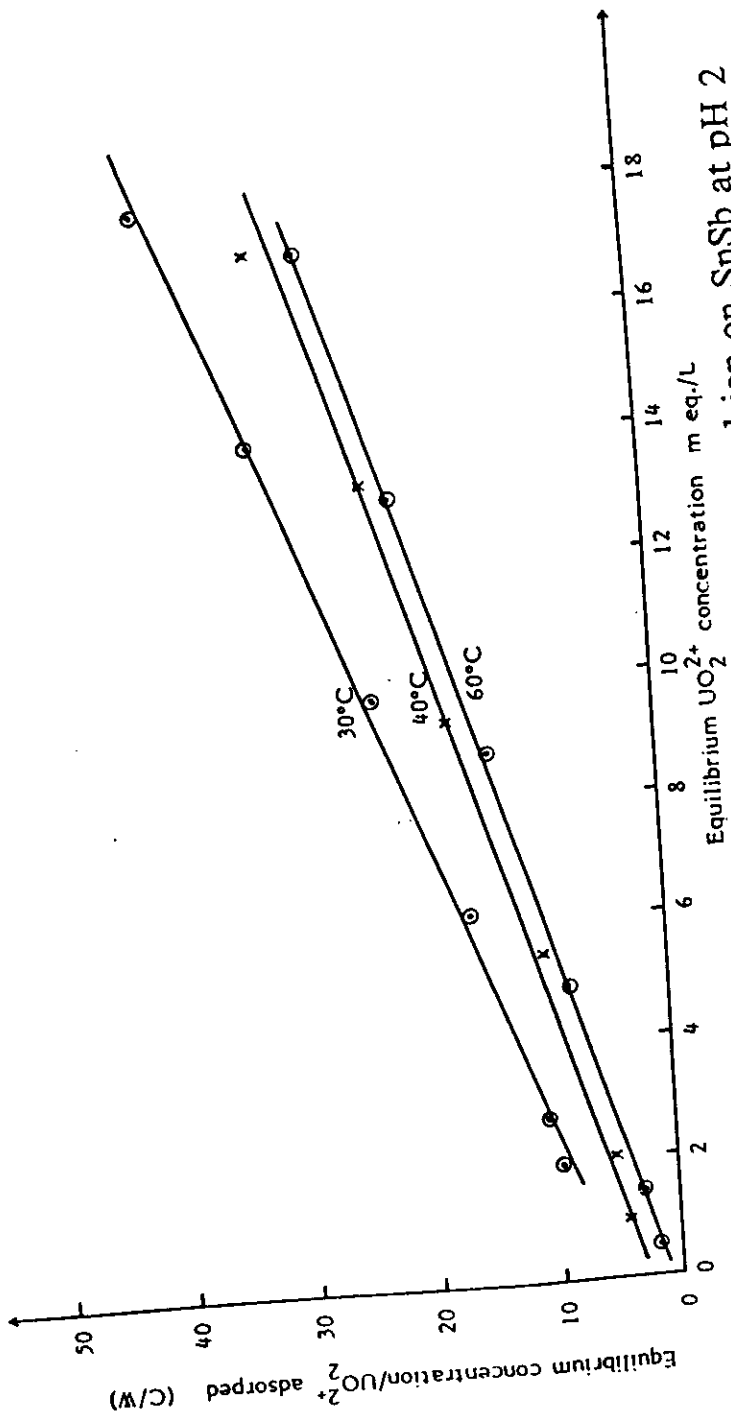

Fig. 24: Langmuir adsorption isotherm of uranyl ion on SnSb at pH 2

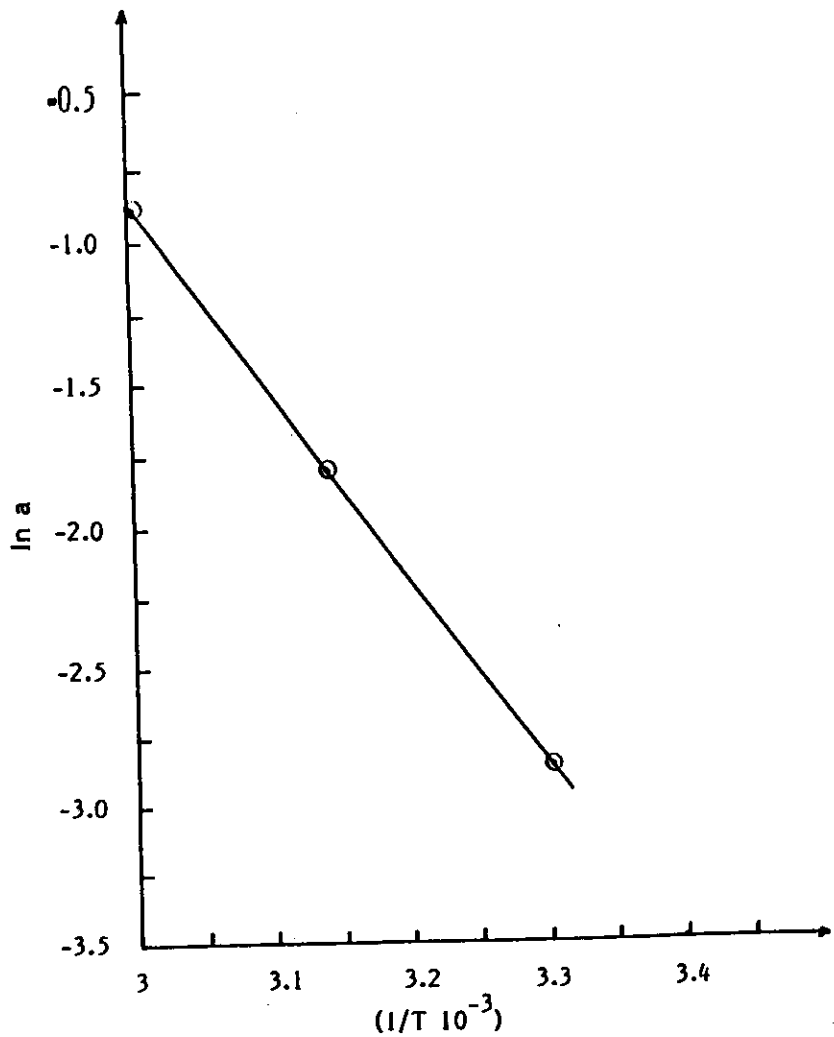

Fig. 25: Plot of ln a vs. 1/T for uranyl ion adsorption on SnSb at pH 2.

7- Europium:

7.1- Distribution coefficient:

The plot of $\log K_d$ vs. $[HNO_3]$ showed that the slope of the straight line obtained is about the same as the valency of the metal ion studied indicating the ideal ion exchange reaction Figure 26. (Appendix I)

7.2- Kinetics of exchange:

The influence of particle radius and solution concentration on the rate of exchange of Eu^{3+} is markedly dependent on the particle size and independent of concentration in the range studied, indicating a particle diffusion controlled exchange of Eu^{3+} ion [230,231].

To verify the particle diffusion controlled mechanism the relation of Bt vs. t, Figures 27,28, and B vs. $1/r^2$, Figure 29, give straight lines confirming the proposed mechanism [231,232]. The results given in Figure 27, shows that the exchange rate increases with the decrease in the particle size, whereas the effective diffusion coefficients are approximately constant, Table 7, which is in agreement with the fundamental condition of particle diffusion. The values of D_i Calculated from Figure 27, are given in Table 7.

The effective diffusion coefficient for lithium, sodium, potassium, cesium, uranyl and cobalt ions on the hydrogen form of SnSb are reported [233] and given as {$6.71X10^{-8}$, $8.65X10^{-8}$, $9.89X10^{-8}$, $15.7X10^{-8}$, $3.5X10^{-9}$ and $6.13X10^{-10}$ cm^2 sec^{-1}} respectively,at 30°C. Comparing these values with the corresponding value of Eu^{3+} given in Table 7, it can be deduced that the mobility of cation is dependent on the cationic

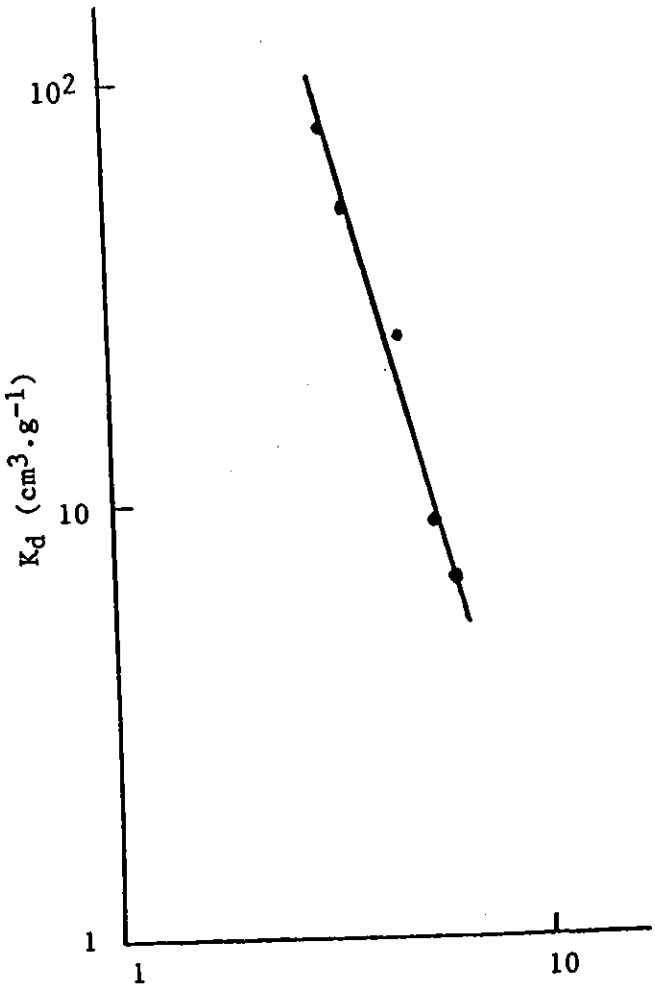

Fig. 26: Plot of K_d vs. nitric acid concentration.

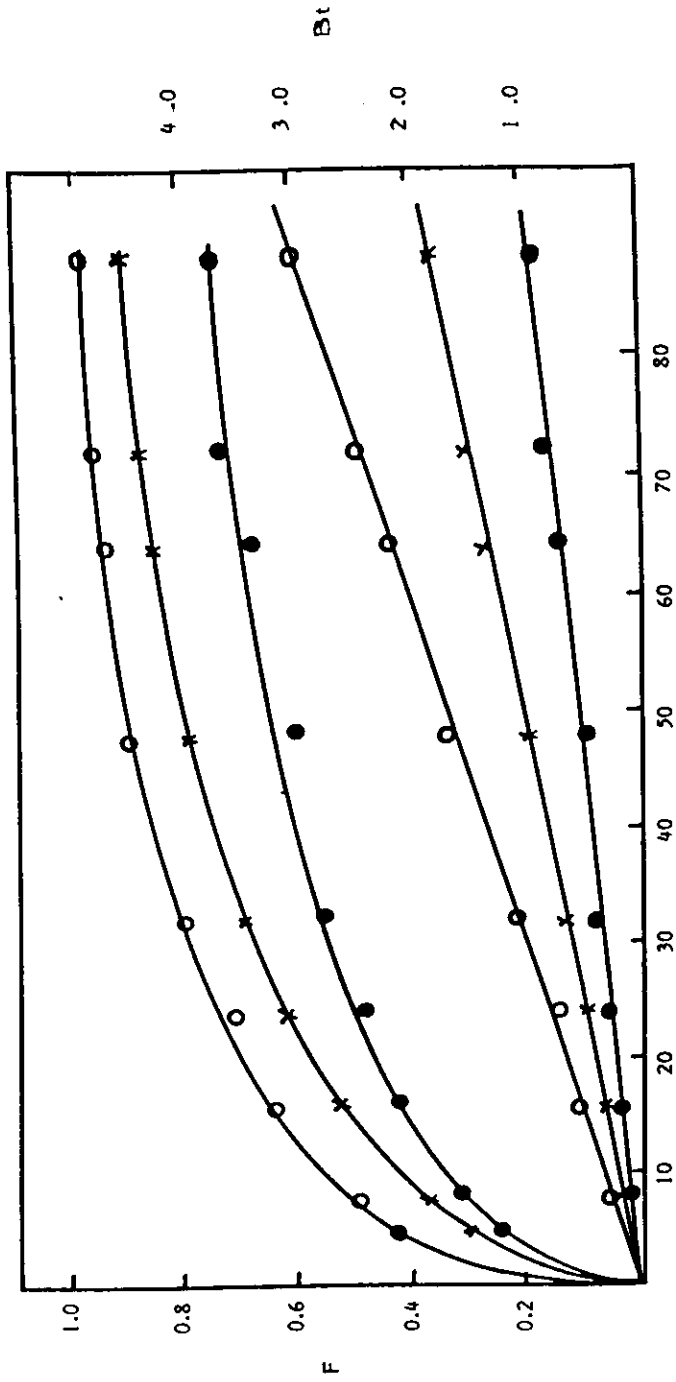

Fig. 27: Plots of F and Bt vs. time for exchange of Eu(III) on SnSb of particle diameter, O, 0.22 mm, X, 0.32 mm; ●, 0.44 mm.

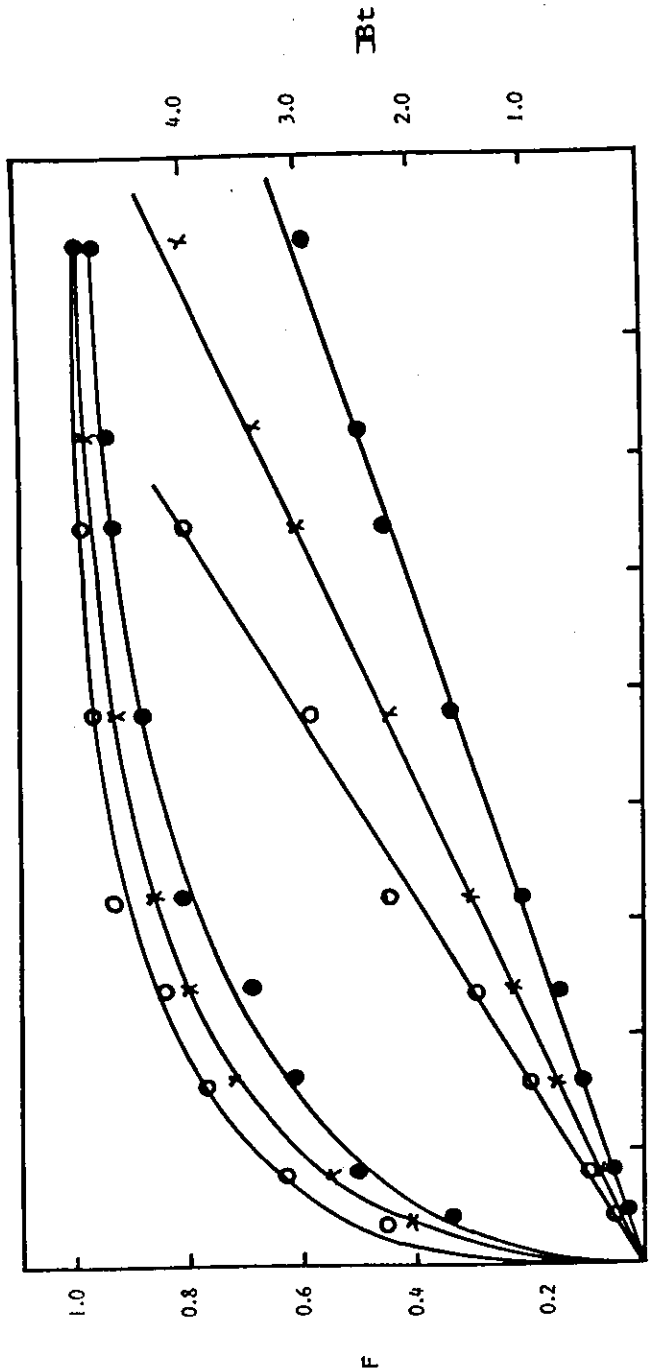

Fig. 28: Plots of F and Bt vs. time for exchange of Eu(III)at different temperature on SnSb of particle diameter 0.16, ●, 25°C; X, 45°C, O, 60°C.

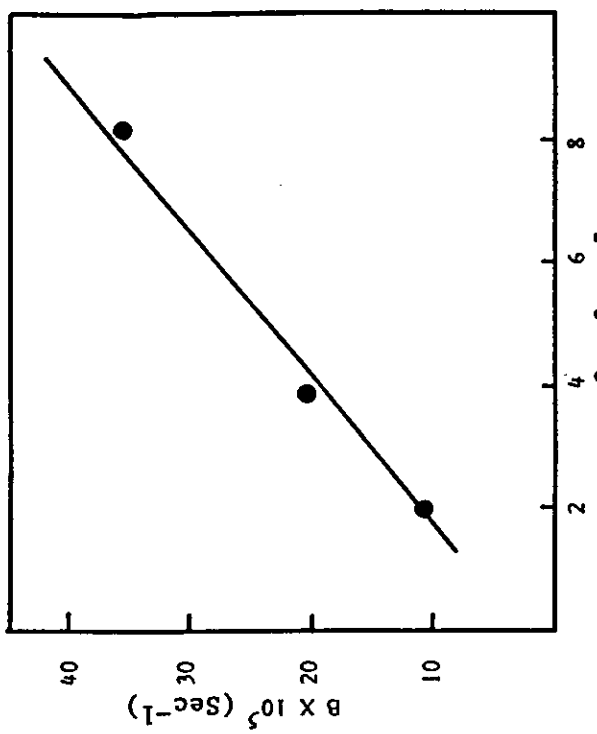

Fig. 29: Plot of B vs. $1/r^2$ for Eu(II)ion at 30°C ion SnSb.

Table 7: Values of D_i at 30°C for Eu^{3+}, at different concentrations, exchange on tin(IV) antimonate of different particle size

Concentration, M	Particle diameter, mm	$D_i X 10^{10}$ $cm^2 Sec^{-1}$
$5X10^{-3}$	0.22	1.24
$8X10^{-3}$	0.22	1.24
10^{-2}	0.22	1.24
10^{-2}	0.32	1.51
10^{-2}	0.44	1.52

exchanger. An analogous behavior was observed for the diffusion of some cations on sulfonic acid resins [231,234] where the mobility was found to be decrease largely with the increase of the charge of the sorbed cations.

Figure 30, shows the values of D_i for the exchange of Eu^{3+} on SnSb for the particle diameter 0.22 mm at the reaction temperatures of 30, 45 and 60°C and recorded in Table 8. The energy of activation E_a, the pre-exponential constant (D_o) and the entropy of activation was calculated from Arrhenius and Barrer equations (Appendix IV).

The value of the diffusion coefficient (D_o), activation energy (E_a) and entropy of activation (ΔS^*) of Eu^{3+} on the H^+ form of SnSb are given in Table 8. The activation energy of the cation diffusion process reflects the case with which cations pass through the exchanger particles. The relatively small activation energy value for euoropium(III) suggests that the rate is particle diffusion controlled [235,236]. The negative values of S^* indicating thereby a certain degree of dehydration of the cation while the diffusion to the solid phase. In addition, a negative value of the entropy of activation suggests that upon exchange of the cation, no significant structural changes occur.

7.3- <u>Sorption isotherm</u>:

The adsorption results were analyzed by the Langmuir adsorption isotherm (Appendix III). A Langmuir plot, Figure 31, shows the conformity of the data with the Langmuir equation. From the slope of the linear plotof C/w vs. C, the adsorption capacity has been determined. The

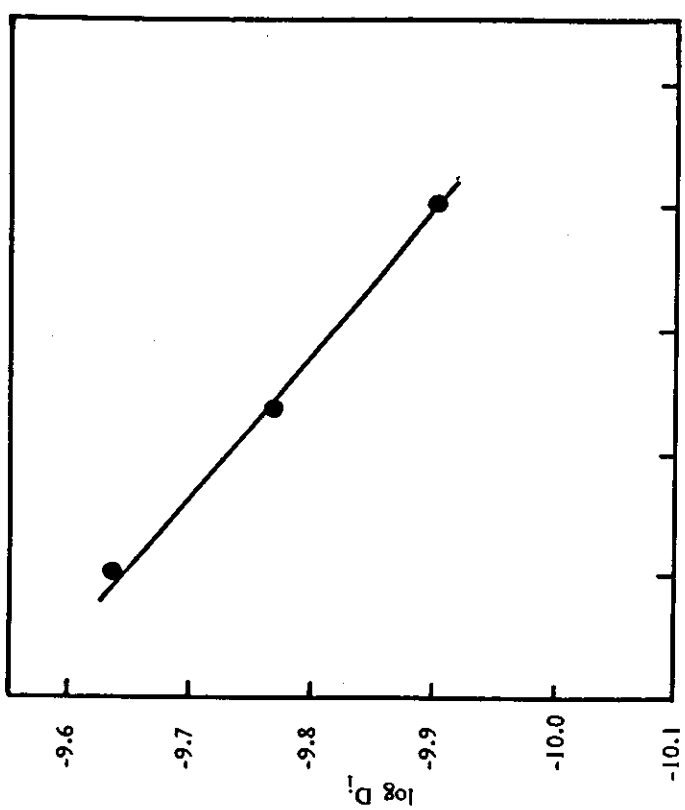

Fig. 30: Arrhenius plot for exchange of Eu(III) ion on SnSb.